Accelerated absorption of regular insulin administered via a vascularizing permeable microchamber implanted subcutaneously in diabetic *Rattus norvegicus*

Short title: Rapid insulin absorption via a subcutaneously implanted microchamber in *R. norvegicus*

Leah V. Steyn[1], Delaney Drew[1], Demetri Vlachos[1], Barry Huey[1], Katie Cocchi[1], Nicholas D. Price[1], Robert Johnson[2], Charles W. Putnam[1], and Klearchos K. Papas[1,2*]

[1]Institute for Cellular Transplantation, Department of Surgery, University of Arizona College of Medicine-Tucson, University of Arizona, Tucson, AZ, USA

[2]Procyon Technologies, LLC., Medical Research Building (Room 121), University of Arizona, Tucson, AZ, USA

*****Corresponding author

Email: kkpapas@surgery.arizona.edu (KPP)

Keywords: insulin, diabetes, microchamber, subcutaneous, rat, absorption, vascularizing, pharmacokinetics

Abstract

In Type 1 diabetes patients, even ultra-rapid acting insulins injected subcutaneously reach peak concentrations in 45 minutes or longer. The lag time between dosing and peak concentration, as well as intra- and inter-subject variability, render prandial glucose control and dose consistency difficult. We postulated that insulin absorption from subcutaneously implantable vascularizing microchambers would be significantly faster than conventional subcutaneous injection. Male athymic nude *R. norvegicus* rendered diabetic with streptozotocin were implanted with vascularizing microchambers (single chamber; 1.5 cm2 surface area per side; nominal volume, 22.5 μL). Plasma insulin was assayed after a single dose (1.5 U/kg) of diluted insulin human (Humulin®R U-100), injected subcutaneously or via microchamber. Microchambers were also implanted in additional animals and retrieved at intervals for histologic assessment of vascularity. Following conventional subcutaneous injection, the mean peak insulin concentration was 22.7 (SD 14.2) minutes. By contrast, when identical doses of insulin were injected via subcutaneous microchamber 28 days after implantation, the mean peak insulin time was shortened to 7.50 (SD 4.52) minutes. Peak insulin concentrations were similar by either route; however, inter-subject variability was reduced when insulin was administered via microchamber. Histologic examination of tissue surrounding microchambers showed mature vascularization on days 21 and 40 post-implantation. Implantable vascularizing microchambers of similar design may prove clinically useful for insulin dosing, either intermittently by needle, or continuously by pump including in “closed loop” systems, such as the artificial pancreas.

Introduction

In response to perturbations of plasma glucose concentration and other physiologic cues, the normal endocrine pancreas modulates its release of insulin (and other hormones); insulin, entering the portal venous circulation in approximately five second pulses and longer oscillations, rapidly and precisely maintains glucose homeostasis [1]. In Type 1 diabetes mellitus (T1DM), the endocrine pancreas fails to produce insulin in sufficient quantities, if at all [2]. Although pharmacologic insulins are a life-saving therapy, they fail to mimic the rapidity and precision of glucose modulation conferred by the normal pancreas [3]. Consequently, despite insulin therapy, diabetic patients remain vulnerable to a range of costly, long-term, disabling complications.

Pharmacologic insulins are most often injected into the subcutaneous (SC) tissue of the abdominal wall or extremities; however, because of the relative avascularity of SC tissue [4], the dispensed insulin - depending upon its formulation - may require an hour or longer to attain its peak concentration in the blood [4]. This delay in absorption renders insulin therapy an exercise in predictive dosing, especially when anticipating the substantial swings in blood glucose concentration encountered during and following meals [5]. The lag time between SC dosing and achieving an effective insulin concentration in the blood also blunts the precision otherwise afforded by continuous glucose monitoring (CGM) devices, sophisticated dosing decision algorithms, precision insulin pumps, open- or closed-loop systems, and the “artificial pancreas” [4, 6].

Efforts to accelerate absorption of insulin have pursued two general approaches: novel formulations of pharmacologic insulins and altered routes of administration. One or more amino acid changes of the insulin molecule itself [7-12] and/or the addition of chemicals [13] reduce the tendency of native insulin to form multimeric complexes which first must dissociate into monomers

or dimers in order to be absorbed [14]. These modifications of pharmacologic insulin have yielded only incremental increases in the rate of absorption (reviewed in [4, 15]). Consequently, ultra-rapid insulins have not achieved wide-spread patient acceptance [4], in part because of increased drug costs [15] and a greater frequency of injection site reactions [16].

The second approach – alternative routes of administration affording more rapid uptake of insulin - have included intradermal microinjection [17] or "jet spray" [18, 19], intraperitoneal instillation [20, 21], or the inhalation of specially formulated insulins [22, 23]. None of these strategies has gained widespread clinical acceptance, in part because of unpredictable dosing, increased complication rates, and patient hesitancy [24, 25].

Although the lag times between SC injection and peak time (T_{max}) have been somewhat foreshortened by the development of "ultra-rapid acting insulins" [Faster aspart (Fiasp), 63 min, URLj (Lyumjev), 57 min [15]], the subcutaneous route is beleaguered by a second confounding problem: intra-patient variability of absorption of the specified dose [26-28] resulting in unanticipated blood glucose effects. This variance between anticipated and actual effect upon blood glucose concentration contributes to the incidence of both diabetic ketoacidosis (DKA) and importantly, hypoglycemic episodes [6], especially in those individuals who are constitutively "hypoglycemia unaware" [29, 30].

Unpredictable discrepancies between the intended and evinced biochemical effects of a particular SC dose are multifactorial. The vascularity of the subcutaneous space is not homogenous even within individuals [22, 31-35] and the SC composition is further altered by repeated injections [36, 37]. In a 2018 review [38], the multitude of factors affecting absorption of SC insulin are discussed in detail; they include, among many others: variations in the depth of needle penetration, including inadvertent intramuscular injection; dislodged catheters or mechanical issues associated

with insulin pump infusion sets [39]; and seepage of drug from the injection site. It stands to reason that intra-patient variability compounds inter-patient dosage algorithms; predictions and comparisons are therefore fraught, requiring complex modeling [40, 41].

To address the challenges posed by lagging absorption of even ultra-fast insulins and the inconsistency of intrasubject dosing, we evaluated in a diabetic *R. norvegicus* model, subcutaneously implantable vascularizing microchambers, IVMs (Fig 1A). These microchambers – of various footprints and capacities – are engineered of polytetrafluoroethylene membranes (PTFE) and have a surface configuration which promotes angiogenic ingrowth; an inner membrane simultaneously blocks host cells from entering and occupying the microchamber [42]. We report here that the IVM, implanted in the SC space, accelerates the absorption of inexpensive regular human insulin, achieving pharmacokinetic profiles potentially superior to ultra-rapid acting insulins. Importantly, our data also suggest that the IVM improves consistency of insulin delivery, thereby potentially avoiding hazardous deviations in blood glucose concentration.

Fig 1. The Procyon implantable vascularizing microchamber (IVM) and an illustrative clinical application.

(A) The vascularizing, microchamber (depicted before implantation), fabricated of PTFE, has a surface area per side of 1.5 cm^2 and a nominal volume of 22.5μL. (B) One potential clinical application of the IVM is to couple it with an insulin pump. The *infusion set* connects the *insulin pump* to the SC implanted *microchamber*; the IVM's *connection tubing* is fitted with a *heal in place cuff* fabricated from material that promotes vascularization. (C) A schematic of the vascularized microchamber, depicting the ingrowth of blood vessels to its surface and the flow of insulin from

within the microchamber, through the permeable membranes, and into the richly vascularized SC space surrounding the IVM.

Materials and methods

Experimental animals

Male athymic nude *R. norvegicus* between 9 - 12 weeks of age and weighing 250 - 350 g were purchased from Envigo (Livermore, CA, USA). Animals were housed for a seven-day acclimatization period before initiating any experimental procedures. All experiments were performed with the approval of, and in accordance with guidelines established by, the Institutional Animal Care and Use Committee (IACUC) at The University of Arizona.

Induction of diabetes

To avoid endogenous insulin in subject rats from cross-reacting in the human insulin assays, animals were rendered diabetic by a single intraperitoneal injection, 60 mg/kg, of streptozotocin (Sigma-Aldrich, St. Louis, MO, USA). Blood glucose concentrations were monitored daily using a Freestyle Lite Glucose Monitoring System (Abbott Diabetes Care Inc., Alameda, CA, USA). Rats were considered diabetic when blood glucose concentrations greater than 200 mg/dL were recorded on three consecutive days. Rats verified as diabetic were maintained with exogenous long-acting insulin (Lantus, Sanofi-Aventis, Bridgewater, NJ, USA) throughout the study; maintenance insulin treatment also serves to forestall insulin resistance [43]. Maintenance insulin therapy was suspended for 24 hours prior to each insulin kinetics study.

Implantation of vascularizing microchambers (IVMs)

Two days after the initial insulin-kinetics assay two empty, 1.5cm^2 per side, single-chamber (having a nominal internal volume of 22.5 μL), implantable vascularizing microchambers, IVMs (Procyon Technologies LLC, Tucson, AZ, USA) (Fig 1A) were implanted subcutaneously on the dorsal aspect of each rat.

Insulin kinetics assays

Subcutaneous injection of human insulin

The initial insulin kinetics assays were performed 7 days after STZ induction of diabetes. Nonfasted rats received a single subcutaneous injection of insulin human, 1.5 U/kg (Humulin R; Lilly, Indianapolis, IN, USA). Each dose of insulin was diluted in 0.5 mL of sterile saline (0.9%) solution, then injected subcutaneously using a glass Hamilton syringe fitted with a 20-gauge sharp needle.

Blood sample collection

Blood samples (150 μL) were collected from the tail vein before injection (time = 0), and at 5-, 15-, 30-, 60-, 90-, and 120-minutes following injection. Blood samples for insulin assays were stored on ice in 1.5 mL centrifuge tubes with EDTA until separation of plasma by centrifugation at 13,300 x g for 15 minutes at 4^o C. Plasma samples were stored at -20^o C.

Administration of human insulin via subcutaneously implanted IVMs

On day 28 post-implantation, each rat received a single dose of insulin human, Humulin R, 1.5 U/kg (Lilly, Indianapolis, IN, USA), diluted as described above. The insulin was then instilled into one of the two IVMs via its port. Blood samples for plasma insulin were collected and processed as described above.

Analysis of rat plasma samples for human insulin concentration

Plasma samples collected from each insulin kinetics assay were analyzed for human insulin concentration using a commercial human insulin ELISA kit (Alpco, Salem, NH, USA). Samples were run in duplicate. The ELISA kit has a detection range of 3.0-200 µIU/mL and a sensitivity of 0.399 µIU/mL. The measured insulin concentrations were converted from IU/mL to µg/mL according to the manufacturer's recommended conversion ratios of 1 IU of human insulin = 6nmol = 34.8 µg of insulin.

IVM retrieval and histopathology

At the conclusion of the study (day 40), rats were euthanized, and the IVMs were retrieved for histology. Additional specimens were obtained 7 and 21 days after implantation from rats in a cohort not included in the insulin analyses reported herein. After removal, each IVM including its adherent tissue was placed in 10% neutral buffered formalin for fixation, then processed for paraffin embedding. Paraffin blocks were sectioned and 5µM slices were collected throughout the microchamber. Sections were stained with hematoxylin and eosin and imaged with a Keyence BZ-X710 microscope (Keyence Co, Osaka, Japan).

Statistical analysis

Insulin kinetic curves

The concentrations of human insulin in each rat were normalized to zero by simple subtraction of the variance at t = 0 from all values for that animal. The insulin kinetic curves were created by calculating the mean values and standard deviations at each time point. In several instances, complete plasma insulin concentration data were not obtained for a given rat in a particular assay; if more than three of the seven data points were unavailable, the subject was excluded from analysis. Data from one animal in the subcutaneous injection (control) group was excluded from analysis on that basis.

Peak insulin times and concentrations

The mean peak times (T_{max}) and concentrations of the insulin kinetic assays were obtained as follows: for each subject the greatest plasma insulin concentration was identified, and both the time point (*e.g.*, 10 min) and the insulin concentration at that time point were tabulated. The mean and SD for each category were then calculated. The two assays, subcutaneous injection at day -2, and IVM administration on day 28, were compared by the unpaired, two-tailed, t-test. The full kinetic curves were compared with the nonparametric Friedman's test [44]. Statistical tests were conducted with GraphPad Prism version 9.4.1 for Windows (GraphPad Software, San Diego, California USA, www.graphpad.com).

Results

Insulin-kinetics study after subcutaneous (SC) injection in diabetic rats

Five days after successful induction of STZ diabetes, rats were injected subcutaneously with diluted human insulin (Humulin R), followed by blood sampling for plasma insulin concentration over a two-hour period. Consonant with the extensive literature documenting inter-subject variability

of insulin absorption after SC injection, the individual insulin curves were quite variable in timing and concentration between animals (Fig 2A), with no clear peak by visual inspection (Fig 2C). The mean peak of plasma insulin – T_{max} – was calculated as 22.7 (n=11, SD 14.2, 95% CI 13.18 – 32.27) min post-injection and the peak concentrations averaged 12.3 (SD 3.16) ng/ml (Table 1). In the experiments described above, the Humulin R stock suspension was diluted in 500 uL sterile saline, approximately a 100-fold dilution. Because the rate of insulin absorption directly correlates with the concentration of mono- and dimers, dilution of the stock solution might seem to favor dissociation of multimeric insulin [9, 14]. In another experiment we compared two concentrations – diluted versus stock – of Humulin R insulin after SC injection. The plasma insulin curves did not vary significantly between the two concentrations (unpublished data), confirming that dilution of Humulin R did not *per se* affect its rate of absorption.

Fig 2. Plasma insulin kinetics after either SC or IVM injection of regular insulin.

Plasma concentrations of human insulin were collected over 120 minutes following either subcutaneous injection (A,C) or instillation into subcutaneous IVMs 28 days after implantation (B,D) of regular insulin human (Humulin R) in identical doses. Shown in A and B are the data for the individual subjects in each group of rats; in C and D are the insulin kinetic curves generated by plotting means and standard deviations (SD). N=11 rats in the SC injection group (one rat was excluded from the analysis because of incomplete plasma insulin concentration data); N=12 rats in the IVM group.

Table 1. Mean peak times and concentrations of plasma insulin after subcutaneous or IVM injection in diabetic rats of insulin human (1.5 U/kg body weight).

	Subcutaneous injection	IVM injection on day 28
Number of subjects (n)	11	12
Body weight (g)	302.1 (SD 25.1)	364.9 (SD 29.6)
T_{max} (min)	22.7 (SD 14.2)	7.50 (SD 4.52) **
95% CI of T_{max} (min)	13.18 – 32.27	4.626 – 10.39
Insulin concentration (ng/ml)	12.3 (SD 3.16)	11.7 (SD 4.97) NS

Given are means, standard deviations (SD), and 95% Confidence Intervals (CI). Although the peak concentrations are not significantly different (NS), the interval to peak concentration (T_{max}) was significantly shorter (** p=0.0020, by the unpaired, two-tailed t test) when insulin was delivered via microchamber.

Insulin kinetics after administration via a subcutaneous microchamber

The implantable vascularizing microchamber (IVM) by Procyon (Fig 1A) is designed to provide a means for rapid, consistent absorption of insulin without repeated needle (or pen or pump cannula) injections; it measures 1.5 cm^2 in surface area per side. Its surface is engineered to promote rapid vascularization. Published reports suggested that to be effectively vascularized, subcutaneously implanted devices typically require three to four weeks in mice [45, 46], two to four weeks in rats [47], and two months or less in primates [48]. We therefore conducted the insulin kinetics assays at 28 days after implantation, anticipating mature vascularization by that time. Diluted insulin human

was instilled into the IVM at the same dose by body weight as in the SC injection control studies, described above.

At 28 days after implantation, 10 of the 12 individual plasma insulin curves peaked just five minutes after injection (Fig 2B), as did the mean value (Fig 2D). The T_{max} for insulin (Table 1) was calculated as 7.50 (SD 4.52, 95% CI 4.626–10.37) min versus 22.7 (SD 14.2) min with conventional SC injection, a statistically significant difference ($p = 0.0020$, Table 1). Not only was uptake of insulin from the microchamber accelerated but the inter-subject variability appeared reduced (Fig 2B); this was also attested by the standard deviations of the mean peak (Table 1) and of the early time points of the insulin curve (Fig 2D). Together, the data at day 28 after implantation, indicate that insulin absorption from the IVM is significantly accelerated with improved inter-subject consistency, compared to conventional SC needle injection.

Evidence of vascularization revealed by histopathology of retrieved IVMs

The peak insulin data presented in the preceding section strongly support the notion that vascularization of the SC tissues surrounding and invading the vascularizing membranes of the microchambers had matured by 28 days and had thereby facilitated the very rapid uptake of insulin. If so, histologic evidence of blood vessels immediately adjacent to the microchambers is likewise expected in the same time frame.

To examine this supposition, IVMs implanted subcutaneously in rats for 7, 21 and 40 days were retrieved and examined histologically. Although the 1.5 cm^2 microchambers were identical to the ones used for insulin kinetics studies, they had not been injected with insulin to avoid

confounding effects on morphology that might be induced by the diffusion of human insulin into the surrounding rat subcutaneous tissues. At 7 days after implantation (Fig 3A) a few vessels can be identified but by day 21, subcutaneous vessels in proximity to the vascularizing membranes are both prominent and plentiful (Fig 3B). Images of subcutaneous tissue surrounding the microchambers at 40 days (Fig 3C-F) reveal the presence of mature vasculature structures with larger vessels quite close to the inner membranes of the IVMs. There was no histologic evidence of fibrotic overgrowth, even at the latest time point. Thus, the histopathology of explanted IVMs indicates that vascularization begins soon after implantation; the numbers of blood vessels greatly increase by three to about six weeks after implantation, an observation congruent with the increased rapidity of insulin uptake on day 28.

Fig 3. Histopathologic images of retrieved microchambers and the surrounding subcutaneous tissues

The images of H & E (hematoxylin and eosin)-stained sections, using 20X (A-C) and 40X (D-F) objectives, of IVMs retrieved 7, 21 or 40 days after implantation. The arrows point to vascular structures. For orientation purposes, the image in C is labeled to identify the *surrounding* (SC) *tissue* and the *insulin delivery chamber*. The linear structure (gray) is the inner membrane of the IVM.

Discussion

Here we report that a small (1.5 cm^2 surface area per side), specially engineered PTFE, vascularizing microchamber (Fig 1) implanted subcutaneously facilitates more rapid uptake of

insulin than conventional SC injection. The IVM recruits the growth of blood vessels which establish a surrounding vasculature, which fully matures by about one month (Fig 3). Regular insulin human (Humulin R), when instilled into the IVM 28 days after implantation, achieves peak plasma concentrations significantly faster than an identical dose delivered by conventional SC injection, 7.50 versus 22.7 min (Fig 2, Table 1). Additionally, inter-subject variability was reduced (Fig 2A,B). We therefore conclude that the subcutaneously implanted microchambers are functionally mature within weeks, not months.

The subcutaneous space is favored for insulin injection for patient convenience: it is a large space readily accessible for injection and easily examined for problems at the sites of skin penetration. Physiologically, however, it is less than ideal; its vascularity is both sparse and heterogenous. Moreover, repeated injections may generate inflammation and consequent fibrosis, rendering the microenvironment even less conducive to absorption of injected insulin. Finally, utilizing the SC space for insulin delivery currently requires repeated injections, by needle, pen or pump, their frequency depending upon the chosen insulin formulation(s) and the means of injection.

The primary clinical scenario for which we envisage the IVM achieving clinical utility for T1DM patients (Fig 1) is a conceptual extension of the experiments described in this report – namely, implantation in diabetic patients to facilitate the very rapid uptake of regular insulin. One might argue that accelerating absorption via an IVM is an unnecessary redundancy now that ultra-rapid acting insulins are available. However, the very rapid peak plasma insulin concentrations achieved with regular insulin via IVM more closely mimic the normal human pancreas and are likely superior to even ultra-rapid acting insulins injected SC [16, 49, 50]. The insulin kinetic curves (Fig 2 B, D) are compatible with an “inject-eat continuum” strategy: this would, first, synchronize the insulin peak with the prandial requirement; and second, avoid the pitfalls of inopportune delays of a meal by

simply postponing the injection. As shown in Fig 1, an insulin pump is easily connected to an IVM, ensuring rapid uptake of the pumped insulin; this would allow greater precision in dosing and rapid uptake of prandial boluses. Other challenging clinical scenarios would likewise benefit from rapid uptake of insulin and therefore better glucose control. One example is insulin therapy of diabetics during pregnancy, where precise glucose homeostasis is vital to the well-being, both immediate and long-term, of mother and fetus [51].

Another argument sometimes made is that rapid uptake of insulin confers more risk than benefit, for example, by triggering hypoglycemic episodes. However, the clinical safety and efficacy, especially in post-prandial control, of ultra-rapid acting insulins is now supported by many studies [15, 16, 52, 53]. The factitious “too rapid” assertion also deflects the many advances in continuous glucose monitoring (CGM) devices, insulin dosage-predicting algorithms, precision-dosing insulin pumps, open and closed loop systems, and the “artificial pancreas” (AP) [6]. To this point, a recent, comprehensive review of multiple input AP systems [54], identified two persistent challenges: lag times in acquiring blood glucose concentration data, and delays in absorption of insulin from SC depots. Our study is relevant to the latter concern, which echoes an earlier sentiment: for APs (and similar approaches) to achieve their full potential, the “applied insulin should induce ideally an instantaneous effect” [4]. The IVM potentially offers a clinical means of further closing the gap between insulin dose and blood glucose response.

Conclusion

Regular insulin human instilled into SC implantable vascularizing microchambers (IVMs) implanted 28 days previously in diabetic rats attains mean peak plasma insulin concentrations in 7.5 (SD 4.50) min, versus 22.7 (SD 14.2) min following conventional SC injection. Inter-subject

variability was likewise reduced. Histologically, mature vascularization was evident at 21 and 40 days after implantation, indicating that neovascularization surrounding the IVMs contributed to the rapidity of insulin uptake. We suggest that the implantable vascularizing microchambers reported herein have clinical potential for the painless, repetitive, reproduceable delivery of regular insulin with an absorption rate potentially exceeding that of ultra-rapid acting insulins.

Acknowledgements

The authors wish to acknowledge Chan A. Ion and Jennifer Kitzmann-Miner for their assistance in preparing graphic work.

References

1. Matveyenko AV, Liuwantara D, Gurlo T, Kirakossian D, Dalla Man C, Cobelli C, et al. Pulsatile portal vein insulin delivery enhances hepatic insulin action and signaling. Diabetes. 2012;61(9):2269-79. Epub 20120611. doi: 10.2337/db11-1462. PubMed PMID: 22688333; PubMed Central PMCID: PMCPMC3425431.

2. Linsley PS, Greenbaum CJ, Nepom GT. Uncovering Pathways to Personalized Therapies in Type 1 Diabetes. Diabetes. 2021;70(4):831-41. doi: 10.2337/db20-1185. PubMed PMID: 33741606; PubMed Central PMCID: PMCPMC7980192.

3. Kramer CK, Retnakaran R, Zinman B. Insulin and insulin analogs as antidiabetic therapy: A perspective from clinical trials. Cell Metab. 2021;33(4):740-7. doi: 10.1016/j.cmet.2021.03.014. PubMed PMID: 33826916.

4. Heinemann L, Muchmore DB. Ultrafast-acting insulins: state of the art. J Diabetes Sci Technol. 2012;6(4):728-42. Epub 20120701. doi: 10.1177/193229681200600402. PubMed PMID: 22920797; PubMed Central PMCID: PMCPMC3440142.

5. Luijf YM, van Bon AC, Hoekstra JB, Devries JH. Premeal injection of rapid-acting insulin reduces postprandial glycemic excursions in type 1 diabetes. Diabetes Care. 2010;33(10):2152-5. Epub 20100806. doi: 10.2337/dc10-0692. PubMed PMID: 20693354; PubMed Central PMCID: PMCPMC2945151.

6. Domingo-Lopez DA, Lattanzi G, L HJS, Wallace EJ, Wylie R, O'Sullivan J, et al. Medical devices, smart drug delivery, wearables and technology for the treatment of Diabetes Mellitus. Adv Drug Deliv Rev. 2022;185:114280. Epub 20220408. doi: 10.1016/j.addr.2022.114280. PubMed PMID: 35405298.

7. Becker RH, Frick AD, Burger F, Scholtz H, Potgieter JH. A comparison of the steady-state pharmacokinetics and pharmacodynamics of a novel rapid-acting insulin analog, insulin glulisine, and regular human insulin in healthy volunteers using the euglycemic clamp technique. Exp Clin Endocrinol Diabetes. 2005;113(5):292-7. doi: 10.1055/s-2005-865637. PubMed PMID: 15926116.

8. Bode BW. Comparison of pharmacokinetic properties, physicochemical stability, and pump compatibility of 3 rapid-acting insulin analogues-aspart, lispro, and glulisine. Endocr Pract. 2011;17(2):271-80. doi: 10.4158/ep10260.Ra. PubMed PMID: 21134878.

9. Brange J, Ribel U, Hansen JF, Dodson G, Hansen MT, Havelund S, et al. Monomeric insulins obtained by protein engineering and their medical implications. Nature. 1988;333(6174):679-82. doi: 10.1038/333679a0. PubMed PMID: 3287182.

10. Mudaliar SR, Lindberg FA, Joyce M, Beerdsen P, Strange P, Lin A, et al. Insulin aspart (B28 asp-insulin): a fast-acting analog of human insulin: absorption kinetics and action profile compared with regular human insulin in healthy nondiabetic subjects. Diabetes Care. 1999;22(9):1501-6. doi: 10.2337/diacare.22.9.1501. PubMed PMID: 10480516.

11. Sheldon B, Russell-Jones D, Wright J. Insulin analogues: an example of applied medical science. Diabetes Obes Metab. 2009;11(1):5-19. doi: 10.1111/j.1463-1326.2008.01015.x. PubMed PMID: 19120431.

12. Vajo Z, Fawcett J, Duckworth WC. Recombinant DNA technology in the treatment of diabetes: insulin analogs. Endocr Rev. 2001;22(5):706-17. doi: 10.1210/edrv.22.5.0442. PubMed PMID: 11588149.

13. Kildegaard J, Buckley ST, Nielsen RH, Povlsen GK, Seested T, Ribel U, et al. Elucidating the Mechanism of Absorption of Fast-Acting Insulin Aspart: The Role of Niacinamide. Pharm Res. 2019;36(3):49. Epub 20190211. doi: 10.1007/s11095-019-2578-7. PubMed PMID: 30746556; PubMed Central PMCID: PMCPMC6373292.

14. Brange J, Owens DR, Kang S, Vølund A. Monomeric insulins and their experimental and clinical implications. Diabetes Care. 1990;13(9):923-54. doi: 10.2337/diacare.13.9.923. PubMed PMID: 2226110.

15. Wong EY, Kroon L. Ultra-Rapid-Acting Insulins: How Fast Is Really Needed? Clin Diabetes. 2021;39(4):415-23. doi: 10.2337/cd20-0119. PubMed PMID: 34866783; PubMed Central PMCID: PMCPMC8603316.

16. Heise T, Piras de Oliveira C, Juneja R, Ribeiro A, Chigutsa F, Blevins T. What is the value of faster acting prandial insulin? Focus on ultra rapid lispro. Diabetes Obes Metab. 2022. Epub 20220519. doi: 10.1111/dom.14773. PubMed PMID: 35593434.

17. Narayan RJ. Transdermal delivery of insulin via microneedles. J Biomed Nanotechnol. 2014;10(9):2244-60. doi: 10.1166/jbn.2014.1976. PubMed PMID: 25992456.

18. Malone JI, Lowitt S, Grove NP, Shah SC. Comparison of insulin levels after injection by jet stream and disposable insulin syringe. Diabetes Care. 1986;9(6):637-40. doi: 10.2337/diacare.9.6.637. PubMed PMID: 3542456.

19. Pehling GB, Gerich JE. Comparison of plasma insulin profiles after subcutaneous administration of insulin by jet spray and conventional needle injection in patients with insulin-dependent diabetes mellitus. Mayo Clin Proc. 1984;59(11):751-4. doi: 10.1016/s0025-6196(12)65585-2. PubMed PMID: 6387316.

20. Dirnena-Fusini I, Åm MK, Fougner AL, Carlsen SM, Christiansen SC. Physiological effects of intraperitoneal versus subcutaneous insulin infusion in patients with diabetes mellitus type 1: A systematic review and meta-analysis. PLoS One. 2021;16(4):e0249611. Epub 20210413. doi: 10.1371/journal.pone.0249611. PubMed PMID: 33848314; PubMed Central PMCID: PMCPMC8043377.

21. van Dijk PR, Logtenberg SJ, Gans RO, Bilo HJ, Kleefstra N. Intraperitoneal insulin infusion: treatment option for type 1 diabetes resulting in beneficial endocrine effects beyond glycaemia. Clin Endocrinol (Oxf). 2014;81(4):488-97. Epub 20140728. doi: 10.1111/cen.12546. PubMed PMID: 25041605.

22. Al-Tabakha MM. Future prospect of insulin inhalation for diabetic patients: The case of Afrezza versus Exubera. J Control Release. 2015;215:25-38. Epub 20150726. doi: 10.1016/j.jconrel.2015.07.025. PubMed PMID: 26222134.

23. Boss AH, Petrucci R, Lorber D. Coverage of prandial insulin requirements by means of an ultra-rapid-acting inhaled insulin. J Diabetes Sci Technol. 2012;6(4):773-9. Epub 20120701. doi: 10.1177/193229681200600406. PubMed PMID: 22920801; PubMed Central PMCID: PMCPMC3440146.

24. Bally L, Thabit H, Hovorka R. Finding the right route for insulin delivery - an overview of implantable pump therapy. Expert Opin Drug Deliv. 2017;14(9):1103-11. Epub 20161207. doi: 10.1080/17425247.2017.1267138. PubMed PMID: 27911116; PubMed Central PMCID: PMCPMC5581917.

25. Spaan N, Teplova A, Stam G, Spaan J, Lucas C. Systematic review: continuous intraperitoneal insulin infusion with implantable insulin pumps for diabetes mellitus. Acta Diabetol. 2014;51(3):339-51. Epub 20140305. doi: 10.1007/s00592-014-0557-3. PubMed PMID: 24595518.

26. Heinemann L. Variability of insulin absorption and insulin action. Diabetes Technol Ther. 2002;4(5):673-82. doi: 10.1089/152091502320798312. PubMed PMID: 12450450.

27. Heise T, Nosek L, Rønn BB, Endahl L, Heinemann L, Kapitza C, et al. Lower within-subject variability of insulin detemir in comparison to NPH insulin and insulin glargine in people with type 1 diabetes. Diabetes. 2004;53(6):1614-20. doi: 10.2337/diabetes.53.6.1614. PubMed PMID: 15161770.

28. Morrow L, Muchmore DB, Ludington EA, Vaughn DE, Hompesch M. Reduction in intrasubject variability in the pharmacokinetic response to insulin after subcutaneous co-administration with recombinant human hyaluronidase in healthy volunteers. Diabetes Technol Ther. 2011;13(10):1039-45. Epub 20110629. doi: 10.1089/dia.2011.0115. PubMed PMID: 21714645.

29. Cryer PE, Davis SN, Shamoon H. Hypoglycemia in diabetes. Diabetes Care. 2003;26(6):1902-12. doi: 10.2337/diacare.26.6.1902. PubMed PMID: 12766131.

30. Fanelli CG, Porcellati F, Pampanelli S, Bolli GB. Insulin therapy and hypoglycaemia: the size of the problem. Diabetes Metab Res Rev. 2004;20 Suppl 2:S32-42. doi: 10.1002/dmrr.514. PubMed PMID: 15551297.

31. Han D, Rahimi E, Aramideh S, Ardekani AM. Transport and Lymphatic Uptake of Biotherapeutics Through Subcutaneous Injection. J Pharm Sci. 2022;111(3):752-68. Epub 20211006. doi: 10.1016/j.xphs.2021.09.045. PubMed PMID: 34624293.

32. Hildebrandt P. Subcutaneous absorption of insulin in insulin-dependent diabetic patients. Influence of species, physico-chemical properties of insulin and physiological factors. Dan Med Bull. 1991;38(4):337-46. PubMed PMID: 1914533.

33. Hildebrandt P. Skinfold thickness, local subcutaneous blood flow and insulin absorption in diabetic patients. Acta Physiol Scand Suppl. 1991;603:41-5. PubMed PMID: 1789128.

34. Hildebrandt PR, Vaag AA. Local skin-fold thickness as a clinical predictor of depot size during basal rate infusion of insulin. Diabetes Care. 1993;16(1):1-3. doi: 10.2337/diacare.16.1.1. PubMed PMID: 8422761.

35. Gradel AKJ, Porsgaard T, Brockhoff PB, Seested T, Lykkesfeldt J, Refsgaard HHF. Delayed insulin absorption correlates with alterations in subcutaneous depot kinetics in rats with diet-induced obesity. Obes Sci Pract. 2019;5(3):281-8. Epub 20190318. doi: 10.1002/osp4.326. PubMed PMID: 31275602; PubMed Central PMCID: PMCPMC6587326.

36. Hajheydari Z, Kashi Z, Akha O, Akbarzadeh S. Frequency of lipodystrophy induced by recombinant human insulin. Eur Rev Med Pharmacol Sci. 2011;15(10):1196-201. PubMed PMID: 22165682.

37. Radermecker RP, Piérard GE, Scheen AJ. Lipodystrophy reactions to insulin: effects of continuous insulin infusion and new insulin analogs. Am J Clin Dermatol. 2007;8(1):21-8. doi: 10.2165/00128071-200708010-00003. PubMed PMID: 17298103.

38. Gradel AKJ, Porsgaard T, Lykkesfeldt J, Seested T, Gram-Nielsen S, Kristensen NR, et al. Factors Affecting the Absorption of Subcutaneously Administered Insulin: Effect on Variability. J Diabetes Res. 2018;2018:1205121. Epub 20180704. doi: 10.1155/2018/1205121. PubMed PMID: 30116732; PubMed Central PMCID: PMCPMC6079517.

39. Kanapka LG, Lum JW, Beck RW. Insulin Pump Infusion Set Failures Associated with Prolonged Hyperglycemia: Frequency and Relationship to Age and Type of Infusion Set During 22,741 Infusion Set Wears. Diabetes Technol Ther. 2022;24(6):396-402. Epub 20220223. doi: 10.1089/dia.2021.0548. PubMed PMID: 35104166.

40. García-Jaramillo M, Calm R, Bondia J, Vehí J. Prediction of postprandial blood glucose under uncertainty and intra-patient variability in type 1 diabetes: a comparative study of three interval models. Comput Methods Programs Biomed. 2012;108(1):224-33. Epub 20120605. doi: 10.1016/j.cmpb.2012.04.003. PubMed PMID: 22677264.

41. Zheng H, Nathan DM, Schoenfeld DA. Using a multi-level B-spline model to analyze and compare patient glucose profiles based on continuous monitoring data. Diabetes Technol Ther. 2011;13(6):675-82. Epub 20110413. doi: 10.1089/dia.2010.0199. PubMed PMID: 21488799; PubMed Central PMCID: PMCPMC3101946.

42. Brauker JH, Carr-Brendel VE, Martinson LA, Crudele J, Johnston WD, Johnson RC. Neovascularization of synthetic membranes directed by membrane microarchitecture. J Biomed Mater Res. 1995;29(12):1517-24. doi: 10.1002/jbm.820291208. PubMed PMID: 8600142.

43. Nordquist L, Sjöquist M. Improvement of insulin response in the streptozotocin model of insulin-dependent diabetes mellitus. Insulin response with and without a long-acting insulin treatment. Animal. 2009;3(5):685-9. doi: 10.1017/s175173110800387x. PubMed PMID: 22444446.

44. Friedman M. The Use of Ranks to Avoid the Assumption of Normality Implicit in the Analysis of Variance. Journal of the American Statistical Association. 1937;32(200):675-701. doi: 10.1080/01621459.1937.10503522.

45. Hussey AJ, Winardi M, Han XL, Thomas GP, Penington AJ, Morrison WA, et al. Seeding of pancreatic islets into prevascularized tissue engineering chambers. Tissue Eng Part A. 2009;15(12):3823-33. doi: 10.1089/ten.TEA.2008.0682. PubMed PMID: 19558221.

46. Pepper AR, Pawlick R, Gala-Lopez B, MacGillivary A, Mazzuca DM, White DJ, et al. Diabetes Is Reversed in a Murine Model by Marginal Mass Syngeneic Islet Transplantation Using a Subcutaneous Cell Pouch Device. Transplantation. 2015;99(11):2294-300. doi: 10.1097/tp.0000000000000864. PubMed PMID: 26308506; PubMed Central PMCID: PMCPMC4623852.

47. Rafael E, Wernerson A, Arner P, Tibell A. In vivo studies on insulin permeability of an immunoisolation device intended for islet transplantation using the microdialysis technique. Eur Surg Res. 1999;31(3):249-58. doi: 10.1159/000008700. PubMed PMID: 10352353.

48. Sasikala M, Rao GV, Vijayalakshmi V, Pradeep R, Pothani S, Kumar PP, et al. Long-term functions of encapsulated islets grafted in nonhuman primates without immunosuppression. Transplantation. 2013;96(7):624-32. doi: 10.1097/TP.0b013e31829e26cf. PubMed PMID: 23883970.

49. Bolli GB, Porcellati F, Lucidi P, Fanelli CG, Owens DR. One-hundred year evolution of prandial insulin preparations: From animal pancreas extracts to rapid-acting analogs. Metabolism. 2022;126:154935. Epub 20211108. doi: 10.1016/j.metabol.2021.154935. PubMed PMID: 34762931.

50. Owens DR, Bolli GB. The continuing quest for better subcutaneously administered prandial insulins: a review of recent developments and potential clinical implications. Diabetes Obes Metab. 2020;22(5):743-54. Epub 20200203. doi: 10.1111/dom.13963. PubMed PMID: 31930670; PubMed Central PMCID: PMCPMC7187182.

51. Amigó J, Corcoy R. Type 1 diabetes and pregnancy: An update on glucose monitoring and insulin treatment. Endocrinol Diabetes Nutr (Engl Ed). 2022. Epub 20220701. doi: 10.1016/j.endien.2022.06.008. PubMed PMID: 35787359.

52. Avgerinos I, Papanastasiou G, Karagiannis T, Michailidis T, Liakos A, Mainou M, et al. Ultra-rapid-acting insulins for adults with diabetes: A systematic review and meta-analysis. Diabetes Obes Metab. 2021;23(10):2395-401. Epub 20210622. doi: 10.1111/dom.14461. PubMed PMID: 34105242.

53. De Block CEM, Van Cauwenberghe J, Bochanen N, Dirinck E. Rapid-acting insulin analogues: Theory and best clinical practice in type 1 and type 2 diabetes. Diabetes Obes Metab. 2022. Epub 20220411. doi: 10.1111/dom.14713. PubMed PMID: 35403348.

54. Hettiarachchi C, Daskalaki E, Desborough J, Nolan CJ, O'Neal D, Suominen H. Integrating Multiple Inputs Into an Artificial Pancreas System: Narrative Literature Review. JMIR Diabetes. 2022;7(1):e28861. Epub 20220224. doi: 10.2196/28861. PubMed PMID: 35200143; PubMed Central PMCID: PMCPMC8914747.

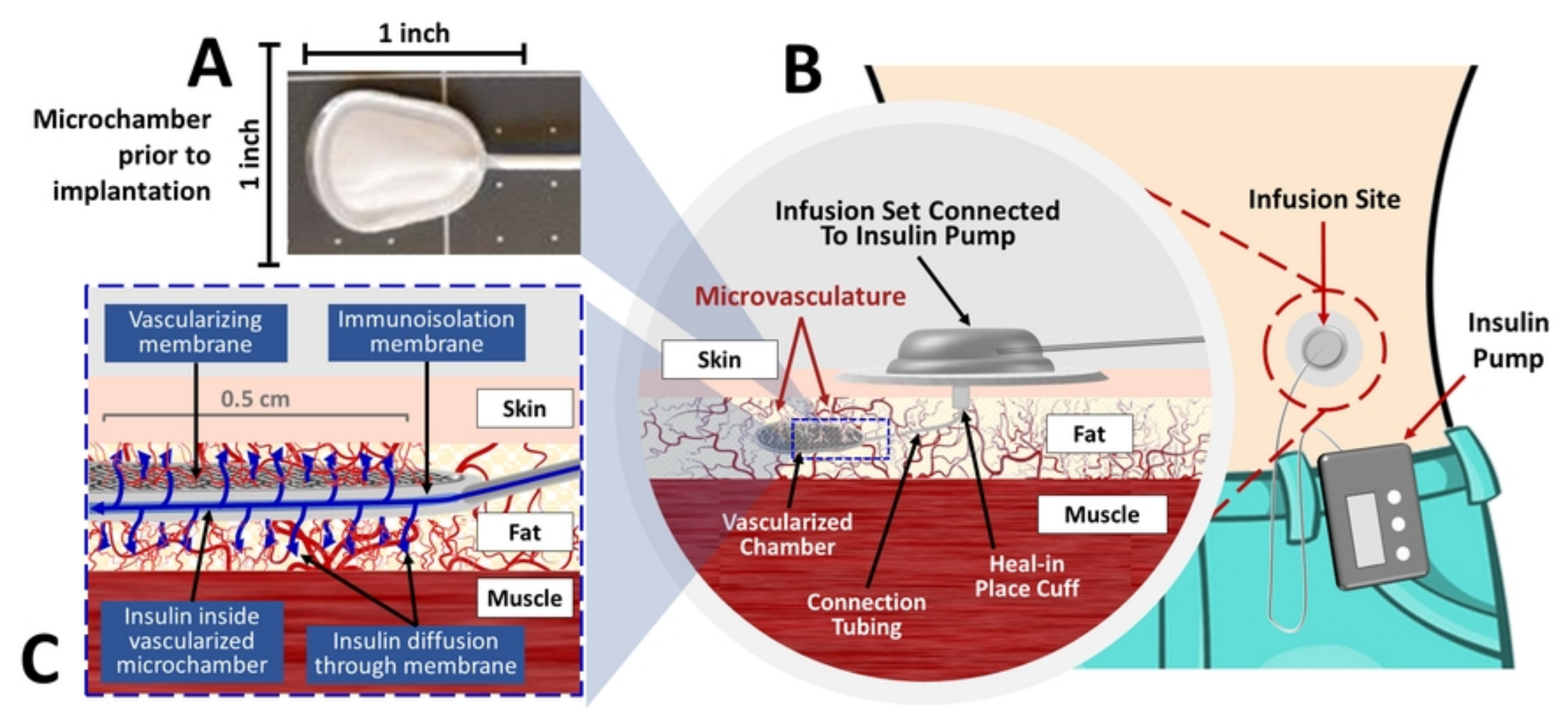
A
1 inch
1 inch
Microchamber prior to implantation
B
Infusion Set Connected To Insulin Pump
Infusion Site
Insulin Pump
Microvasculature
Skin
Fat
Muscle
Vascularized Chamber
Connection Tubing
Heal-in Place Cuff
C
Vascularizing membrane
Immunoisolation membrane
0.5 cm
Skin
Fat
Muscle
Insulin inside vascularized microchamber
Insulin diffusion through membrane

Figure 1

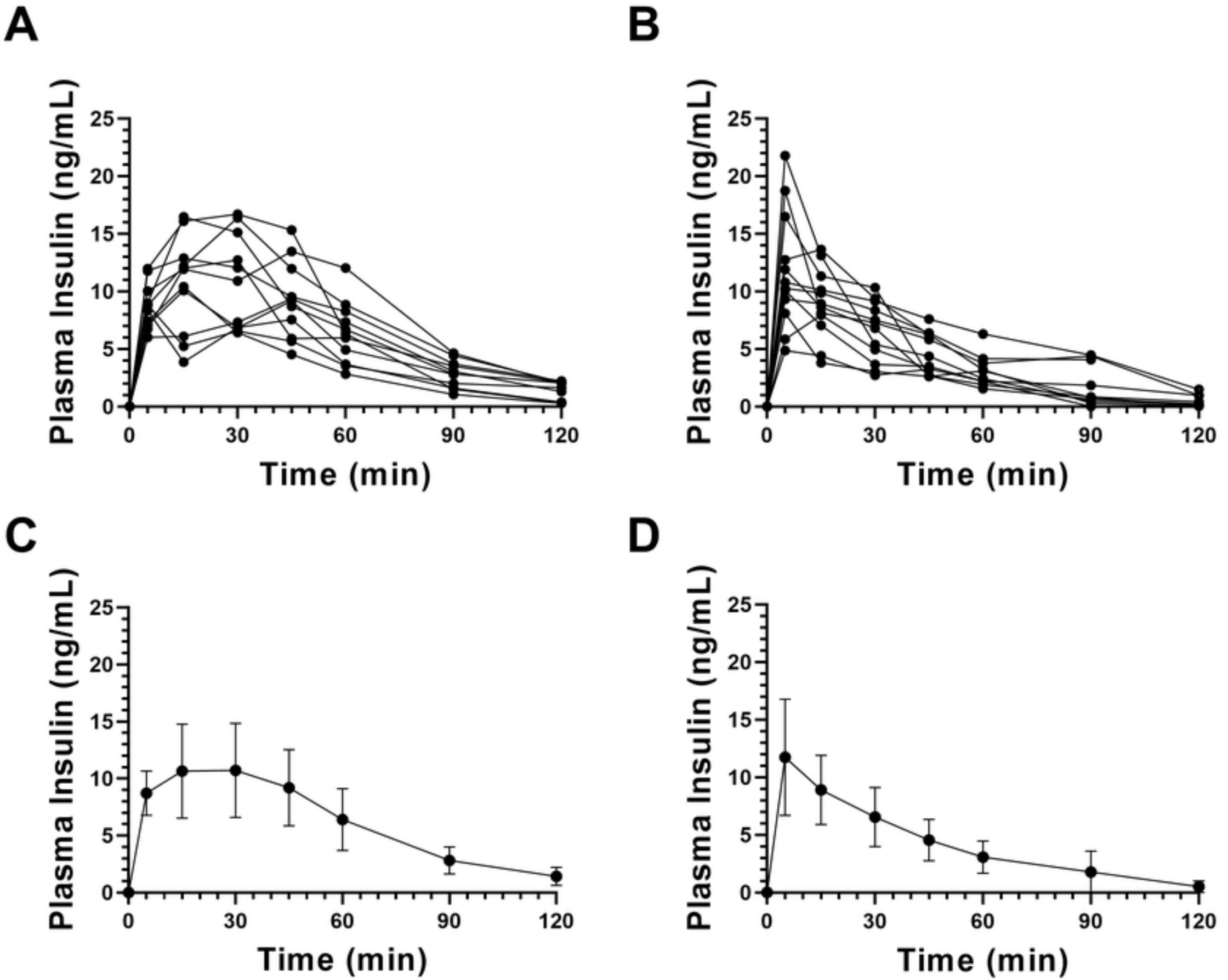

Figure 2

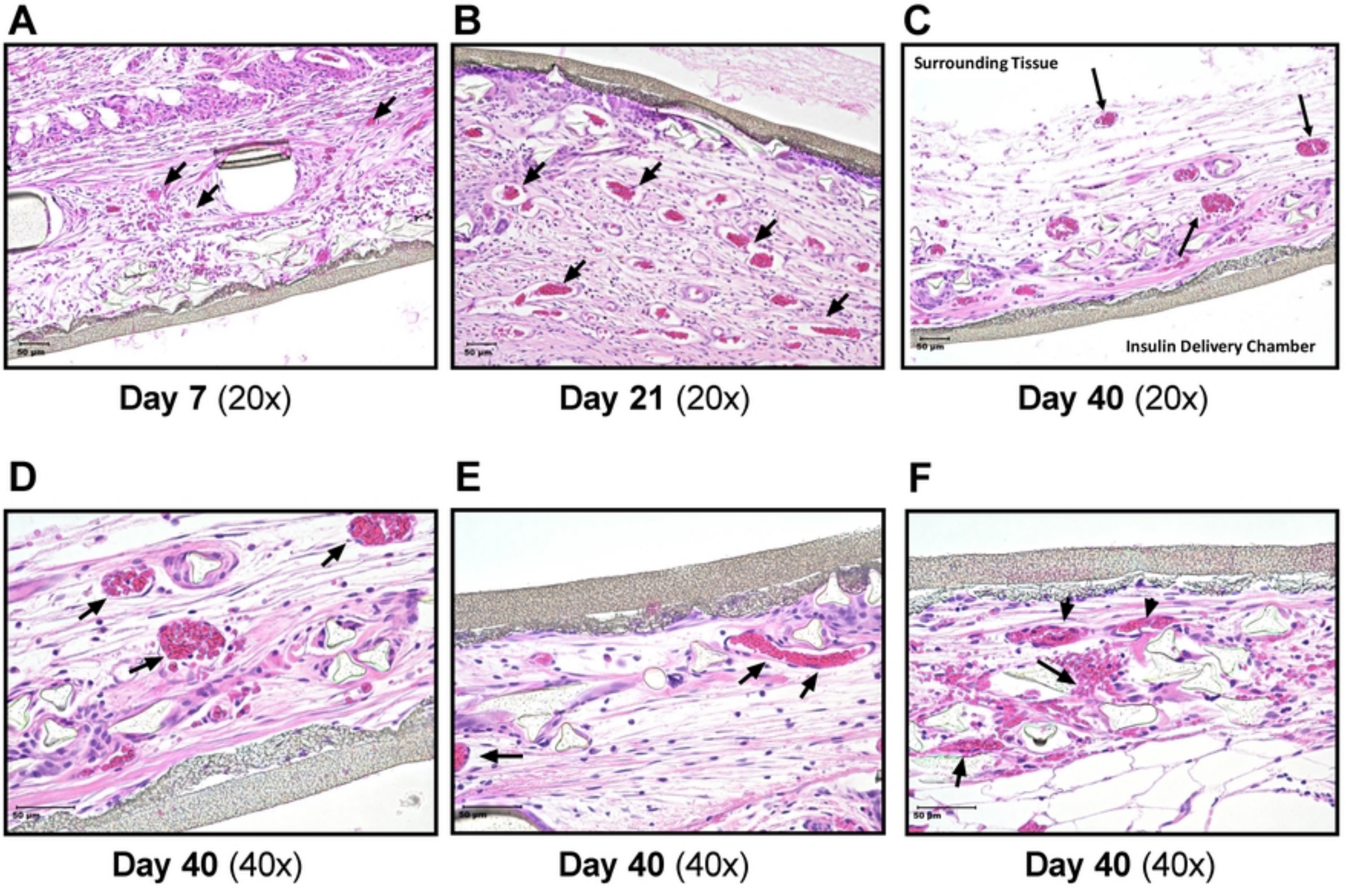
A
B
C
Surrounding Tissue
Insulin Delivery Chamber
Day 7 (20x)
Day 21 (20x)
Day 40 (20x)
D
E
F
Day 40 (40x)
Day 40 (40x)
Day 40 (40x)

Figure 3